Journal of Manufacturing Engineering, ISSN: 0973-6867, December 2024, Vol. 19, Issue. 4, pp 108-125
DOI: https://doi.org/10.37255/jme.v19i4pp108-125

MATHEMATICAL MODELING OF SHAPE RELATIONSHIP INCLUDING % DILUTION AND TOTAL BEAD VOLUME IN SAW PROCESS BY USING TWO LEVEL HALF FACTORIAL TECHNIQUE

***Deepak Kumar Choudhary, Ram Manohar Pandey, Chandra Prakash and Vishwjeet Kumar**

Mechanical Engineering Department, Sandip Foundation, Shri Ram Polytechnic College, Sijoul, Bihar-847235, India

ABSTRACT

The fabrication industry extensively uses SAW (Submerged Arc Welding) owing to its quality, precision and high production rate. The quality and strength of the weld are controlled by the weld bead geometry criterion and shape relationship, which are greatly influenced by the SAW process control variables, namely welding current, arc voltage, welding speed and nozzle-to-plate distance. The present study aims to develop mathematical relations between weld penetration shape factor (WPSF), weld reinforcement form factor (WRFF), % dilution, and total volume with process control variables. Experiments were conducted using "Two Level Half Factorial Design Techniques". Design Expert software was deployed for graph plotting for the primary and interaction effects of process control variables on bead geometry parameters. Results indicated that voltage affects WPSF positively, while welding current and nozzle-to-plate distance affect WPSF negatively, and welding speed has an insignificant effect on WPSF. Similarly, for WRFF, arc voltage and welding speed have a positive effect, while welding current and nozzle-to-plate distance have a negative impact. For % dilution, nozzle-to-plate distance has an adverse effect and welding current has an insignificant impact. Welding current effects, the total bead volume, arc voltage, welding speed, and nozzle-to-plate distance have adverse effects.

Keywords: *Bead geometry, Mathematical model, Response, Two-level half-factorial design technique*

1. Introduction

Welding is a key technology in the fabrication industry because it produces precise, robust, versatile, and adaptable joints. The continual evolution in welding technology guarantees that it will continue to be a crucial catalyst for innovation and industry expansion. Welding is extensively used in today's technology. It has been phenomenally used since about 1930; the growth has been faster than the general industrial growth. SAW is one of the oldest automatic/semiautomatic welding processes introduced in the middle and late 1930s. This process produces very high productivity and excellent weld quality [1,2]. The strength and the quality of the weld are greatly influenced by the bead geometry and shape relationships. The bead geometry parameters are closely related to the welding parameters like welding current, arc voltage, welding speed, and nozzle-to-plate distance. A relationship between welding variables and bead geometry parameters must be established for excellent weld quality and better control of the weld bead geometry parameters. The ongoing trend in the fabrication industry is "automated welding processes" to obtain high precision and production volume. Researchers have sincerely attempted to develop the relationship between SAW's process variables and bead geometry parameters for improved weld quality.

Yang and Bibby [1993] conducted experiments to find the result of bead-on-plate submerged arc welding to determine the effects of process variables on the weld deposit area. Gunraj et al. [2000] studied and analysed various process control variables and important weld bead quality parameters in SAW of manufactured pipes. Kumanan et al. [2007] applied the Taguchi Technique and Regression Analysis to determine the optimal process parameters for submerged arc welding. Tewari et al. [2010] studied the effect of various welding parameters on the weldability of Mild Steel specimens welded by metal arc welding. Deepak et al. [2011] experimented with submerged arc welding by making beads on steel (SS -304) plates to

**Corresponding Author - E- mail: deepak.choudhary@shrirampolytechnic.org*

Journal of Manufacturing Engineering, ISSN: 0973-6867, December 2024, Vol. 19, Issue. 4, pp 108-125
DOI: https://doi.org/10.37255/jme.v19i4pp108-125

investigate the effect of welding parameters on bead geometry. Two-level Half Factorial Design is one of the most widely used types of design for process design and process improvement. The two-level Half Factorial Design technique is one of the most used methods for process design and improvement [3]. The two-level half-factorial design technique reduces experimental costs and provides the required information about the main and the interaction effect of welding parameters on responses [7]. Therefore, a two-level half fractional factorial design (2^{4-1}) = 8 weld runs was selected in the present work to develop mathematical models and to determine the main and interaction effects of welding parameters on bead geometry parameters and shape relationships. This technique gives satisfactory results while investigating the effects of welding parameters on bead geometry in submerged arc welding [4, 12]. The design required two sets of eight weld runs to calculate the mathematical models and the central and interaction effects of process parameters on the responses by Design expert software.

In the present study, an attempt has been made to develop the relationship between the process variables and bead geometry parameters like Weld Penetration Shape Factors (WPSF), Weld Reinforcement Form Factor (WRFF), total bead volume, and percentage dilution through experiments, based on half factorial design technique. The primary and interaction effects of process variables on bead geometry parameters were analyzed and represented with the help of graphs by using Design Expert software. The experiments were conducted on a carbon steel plate (ASTM SA 516 grade 60) by making a bead on the plate. ASTM SA 516 grade 60 carbon steel is extensively used for manufacturing pressure vessels and boilers.

2. Experimentation

2.1 Identification of the Process Variable and Finding their Working Range

The process variables were chosen based on their controllability and impact on bead geometry. Travel speed (S), nozzle-to-plate distance (N), open circuit voltage (V), and welding current (I) were the four independently controlled process variables chosen. By adjusting one process variable at a time while maintaining the values of the others constant, the working range was established through trial and error. The numbers +1 and -1 represented the upper and lower bounds, respectively. The selected process parameters and their upper and lower limits, together with notations and units, are given in Table 1.

Table 1 Welding Parameters with levels

S.No	Parameters	Unit	Symbol	Levels	
				Low (-1)	High (+1)
1	Welding current	Amp	I	250	450
2	Arc Voltage	Volt	V	30	32
3	Welding Speed	m/hr	S	27.4	36.6
4	Nozzle-to-Plate distance	mm	N	20	25

2.2 Development of Design Matrix

Table 2 Design Matrix shown in actual values

S.No.	I	V	S	N = I × V × S
1	450	32	36.6	25
2	250	32	36.6	20
3	450	30	36.6	20
4	250	30	36.6	25
5	450	32	27.4	20
6	250	32	27.4	25
7	450	30	27.4	25
8	250	30	27.4	20

Table 2 displays the design matrix created using the two-level half-factorial design approach, which results in several experiment combinations 2k-1 (2^{4-1} = 8). The connection N = I × V × S produced the fourth column, while the first three were made using the conventional 23 two-level full factorial. Table 2 also shows the design matrix in actual values.

2.3 Conducting Experiment as per Design Matrix

The experiments were carried out on an automatic submerged arc welding machine. A carbon steel plate measuring 150 x 75 x 12 mm was beaded using a constant potential transformer rectifier type power supply with an 800-ampere current capability at a 60% duty cycle and an open circuit voltage of 20 to 50 volts. Agglomerated flux and a coil-shaped, copper-coated electrode AWS 5.17 EL-8 with a 3.2 mm diameter were employed. To prevent any systematic inaccuracy, the experiments were conducted at random. Using Design Expert software, the entire set of eight trials was repeated to calculate the model's adequacy and parameter variance. The 20 mm-long weld samples were removed from the centre of the weld plate and polished using a range of finer emery paper grades (80, 100, 200, 300, 400, 600, 800, and 1000). After the appropriately polished specimens were etched using 2% Nital solution, they were examined and analyzed. Table 3 displays the base plate's chemical makeup.

Journal of Manufacturing Engineering, ISSN: 0973-6867, December 2024, Vol. 19, Issue. 4, pp 108-125
DOI: https://doi.org/10.37255/jme.v19i4pp108-125

Table 3 Chemical Composition of Base Plate

Composition	C	Si	Mn	P	S	Al	Cr	Cu	Ni	Mo	Nb	Ti	V
Percentage	0.2	0.4	1.4	0.03	0.03	0.02	0.3	0.3	0.3	0.8	0.01	0.03	0.02

Table 4 Measured values of bead geometry

S.NO.	Penetration(p)		Reinforcement(h)		Bead width(w)	
	1	2	1	2	1	2
1	3	3.2	2.05	2.1	16.2	16.2
2	1.41	1.5	1.4	1.2	11	11.08
3	3.32	3.39	2.5	2.9	15.7	15.2
4	1.5	1.61	1.64	1.5	11.2	11.42
5	3.77	3.55	2.7	2.52	20.8	21.2
6	1.46	1.58	1.72	1.74	11.62	11.4
7	3.61	3.88	3.2	2.9	12.13	12.42
8	1.52	1.72	1.54	1.62	12.66	12.88

Table 5 Calculated values of bead geometry parameters

Trial No.	WPSF		WRFF		% Dilution		Total bead volume	
	1	2	1	2	1	2	1	2
1	5.4	5.06	7.9	7.71	78.32	**77.22**	620.52	671.37
2	7.8	7.39	7.86	9.23	74.38	87.22	208.52	190.55
3	4.73	4.48	6.28	5.24	65.7	56.54	793.39	911.31
4	7.47	7.09	6.83	7.61	65.05	73.31	258.24	250.8
5	5.52	5.97	7.7	8.41	76.55	81.83	1024.35	919.75
6	7.96	7.22	6.76	6.55	63.3	62.81	268.01	286.78
7	3.36	3.2	3.79	4.28	45.64	51.75	959.35	931.1
8	8.33	7.48	8.22	7.95	76.93	63.29	250.13	350.01

Table 6 Result of ANOVA for WPSF

Source	Sum of Squares	Degree of Freedom	Mean Square	F - Value	P-value Prob > F	Remarks
Model	39.404	4	9.851	57.826	< 0.0001	significant
I - Welding Current	33.102	1	33.103	194.313	< 0.0001	significant
V - Voltage	2.374	1	2.374	13.934	0.0033	significant
N - Nozzle to plate distance	1.531	1	1.531	8.988	0.0121	significant
IV	2.396	1	2.397	14.069	0.0032	significant
Residual	1.874	11	0.17			
Lack of Fit	0.885	3	0.295	2.388	0.1445	not significant
Pure Error	0.989	8	0.124			
Cor Total	41.278	15				

Journal of Manufacturing Engineering, ISSN: 0973-6867, December 2024, Vol. 19, Issue. 4, pp 108-125
DOI: https://doi.org/10.37255/jme.v19i4pp108-125

Table 7 Result of ANOVA for WRFF

Source	Sum of Squares	Degree of Freedom	Mean Square	F - Value	P-valueProb > F	Remarks
Model	31.441	5	6.288	25.729	< 0.0001	significant
I - Welding Current	5.861	1	5.861	23.983	0.0006	significant
V - Voltage	8.884	1	8.884	36.35	0.0001	significant
S - Welding speed	1.564	1	1.564	6.399	0.0299	significant
N - Nozzle to plate distance	5.593	1	5.593	22.88	0.0007	significant
IV	9.539	1	9.539	39.031	< 0.0001	significant
Residual	2.444	10	0.244			
Lack of Fit	0.203	2	0.101	0.362	0.7071	not significant
Pure Error	2.241	8	0.28			
Cor Total	33.885	15				

Table 8 Result of ANOVA for % Dilution

Source	Sum of Squares	Degree of Freedom	Mean Square	F - Value	P-value Prob >F	Remarks
Model	1579.19	4	394.798	11.863	0.0006	significant
V - Voltage	668.177	1	668.177	20.077	0.0009	significant
S - Welding speed	193.453	1	193.453	5.813	0.0346	significant
N - Nozzle to plate distance	264.374	1	264.374	7.944	0.0167	significant
IV	453.187	1	453.187	13.617	0.0036	significant
Residual	366.09	11	33.281			
Lack of Fit	81.356	3	27.119	0.762	0.5464	not significant
Pure Error	284.734	8	35.592			
Cor Total	1945.281	15				

Table 9 Result of ANOVA for Total bead volume:

Source	Sum of Squares	Degree of Freedom	Mean Square	F - Value	P-value Prob > F	Remarks
Model	1550483.639	5	310096.728	96.426	< 0.0001	significant
I - Welding Current	1420925.298	1	1420925.297	441.845	< 0.0001	significant
V - Voltage	16543.739	1	16543.739	5.144	0.0467	significant
S - Welding speed	73546.171	1	73546.171	22.869	0.0007	significant
IS	21838.618	1	21838.618	6.791	0.0262	significant
IN	17629.813	1	17629.813	5.482	0.0412	significant
Residual	32158.932	10	3215.893			
Lack of Fit	12689.622	2	6344.811	2.607	0.1343	not significant
Pure Error	19469.31	8	2433.662			
Cor Total	1582642.572	15				

Journal of Manufacturing Engineering, ISSN: 0973-6867, December 2024, Vol. 19, Issue. 4, pp 108-125
DOI: https://doi.org/10.37255/jme.v19i4pp108-125

Table 10 Model summary statistics for responses

Parameters	Std. Dev.	Mean	C.V %	Press	R-Squared	Adj R-Squared	Pred. R-Square	Adequate Precision
WPSF	0.413	6.154	6.707	3.965	0.955	0.938	0.904	18.504
WRFF	0.494	7.021	7.041	6.257	0.928	0.891	0.815	14.893
% Dilution	5.769	68.741	8.392	774.537	0.812	0.743	0.601	9.829
Total bead volume	56.709	555.886	10.201	82326.867	0.98	0.97	0.948	22.979

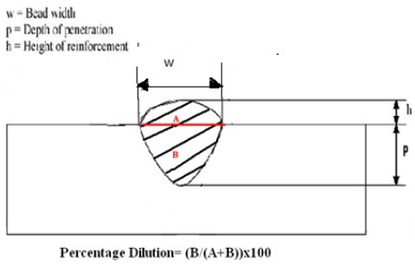

Fig. 1 Actual Bead Geometry

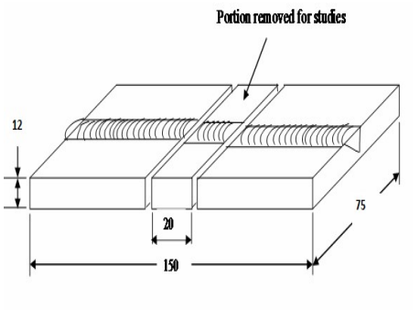

Fig. 2 Cutting plan

2.4 Calculation of Bead Geometry Parameters (Shape Relationship

A circular sector with a radius (p + h) has been considered for the bead cross-section form to calculate the geometry parameters. From simple geometry, the percentage dilution and total bead volume can be readily estimated [9]. Figures 1 and 3 show both the original and updated bead geometry.

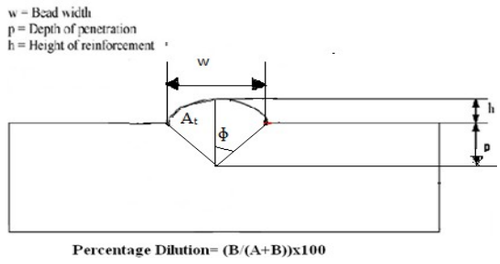

Fig. 3 Simplified Bead Geometry

$A_t = (p + h)^2 \phi$, where ϕ is semi arc angle, in radian. (1)
And $\tan\phi = w/2p$, (ϕ in degree) (2)
WPSF = w/p (3)
WRFF = w/h (4)
% D = $(A_p/A_t) \times 100$ (5)
$A_p = ½(w \times p)$ (6)
$V_t = A_t \times$ width of the specimen (20 mm) (7)

2.5 Selection of Mathematical Model

Any of the weld bead dimensions could be represented by the response function Y = f (I, V, S, N), where Y is the response function such as the total bead volume, the percentage dilution, the weld reinforcement form factor (WRFF), and the weld penetration shape factor (WPSF). I, V, S, and N represent the welding current, arc voltage, welding speed, and nozzle-to-plate distance. The expression above could be stated as follows, assuming a linear relationship in the first place and accounting for conceivable interactions of only two factors.

$Y= b_0+ b_1I + b_2V+ b_3S + b_4N + b_5IV + b_6IS + b_7IN$(8)

Where b0 is constant and b_1, b_2, b_3, b_4, b_5, b_6, b_7 are the coefficients of effects.

2.6 Checking the Significance of the Model

Journal of Manufacturing Engineering, ISSN: 0973-6867, December 2024, Vol. 19, Issue. 4, pp 108-125
DOI: https://doi.org/10.37255/jme.v19i4pp108-125

Based on the investigation of the experimental data, a statistical technique known as ANOVA may reveal specific essential findings. The approach is constructive for determining the degree of importance of a factor's influence or interaction with another factor on a given answer. The statistical significance of the components included in the response factors and the fitted linear models was assessed using the analysis of variance (ANOVA) test. The lack of fit test was used to examine the fitted linear model's goodness of fit. The results obtained are shown in Tables 4-10.

It is decided that every fitted model is significant. Since the probability of F (PROB. >F) for the responses such as WPSF, WRFF, and total bead volume is less than 0.0001, meaning that there is only a 0.01% chance that "Model F-Value" larger could occur due to noise. The probability of F (PROB. >F) for the response %Dilution is 0.0006, indicating that there is only a 0.06% chance that a "Model F-Value" larger could occur due to noise. "Prob > F" values below 0.0500 signify the value of the model terms. The model terms are not significant if the values are higher than 0.1000. In the case of % Dilution and total bead volume, V, S, N, IV and I, V, S, IS, IV are significant model terms, respectively, as are I, V, N, IV and I, V, S, N, and IV in the WPSF and WRFF models. Each model's lack of fit is insignificant compared to the pure error. WPSF, WRFF, % Dilution, and total bead volume had relative chances of 14.45%, 70.71%, 54.64%, and 13.43% that a "LACK OF FIT F-VALUE" bigger could be attributed to noise. A minor mismatch is good.

2.7 Evaluation of the Coefficients of the Models

The design expert software package was used to determine the values of the model's coefficients. The student's t-test assessed each coefficient's significance at the % confidence level of 95%. Coefficients are shown in Table 11-14.

Table 11 Coefficients of Model for WPSF

Factor	Coefficient
Intercept	6.15
I-Welding current	-1.44
V-Voltage	0.39
N-Nozzle to plate distance.	-0.31
IV	0.39

Table 12 Coefficients of Model for WRFF

Factor	Coefficient
Intercept	**7.02**
I-Welding current	**-0.61**
V-Voltage	**0.75**
S-Welding speed	**0.31**
N-Nozzle to plate distance.	**-0.59**
IV	**0.77**

Table 13 Coefficients of Model for % Dilution

Factor	Coefficient
Intercept	**68.74**
V-Voltage	**6.46**
S-Welding speed	**3.48**
N-Nozzle to plate distance.	**-4.06**
IV	**5.32**

Table 14 Coefficients of Model for Total Bead Volume

Factor	Coefficient
Intercept	**555.89**
I-Welding current	**298.01**
V-Voltage	**-32.16**
S-Welding speed	**-67.8**
IS	**-36.94**
IN	**-33.19**

2.8 Development of Mathematical Model

The final mathematical models for the responses are presented in Table 15.

Table 15 Developed Mathematical Models

Responses	Mathematical models
WPSF	6.15 - 1.44 × I + 0.39 × V - 0.31 × N + 0.39 × IV
WRFF	7.02 - 0.61× I + 0.75 × V + 0.31 × S - 0.59 × N + 0.77 × IV
%Dilution	68.74 + 6.46 × V + 3.48 × S - 4.06 × N + 5.32 × IV
Weld Bead Volume	555.89 + 298.01 × I-32.16 × V-67.80 × S-36.94 × IS-33.19 × IN

Journal of Manufacturing Engineering, ISSN: 0973-6867, December 2024, Vol. 19, Issue. 4, pp 108-125
DOI: https://doi.org/10.37255/jme.v19i4pp108-125

3. Analysis of Result and Discussions

The predicted effects of the SAW process variable on the weld bead geometry parameters within the range of the process variables are represented in Fig. 4-27.

3.1 Main Effect of Process Variables on WPSF

Fig. 4-6 It demonstrates that the weld penetration shape factor (WPSF) rises as voltage increases but falls as welding current and nozzle-to-plate distance increase. On the weld penetration shape factor, welding speed has no noticeable impact.

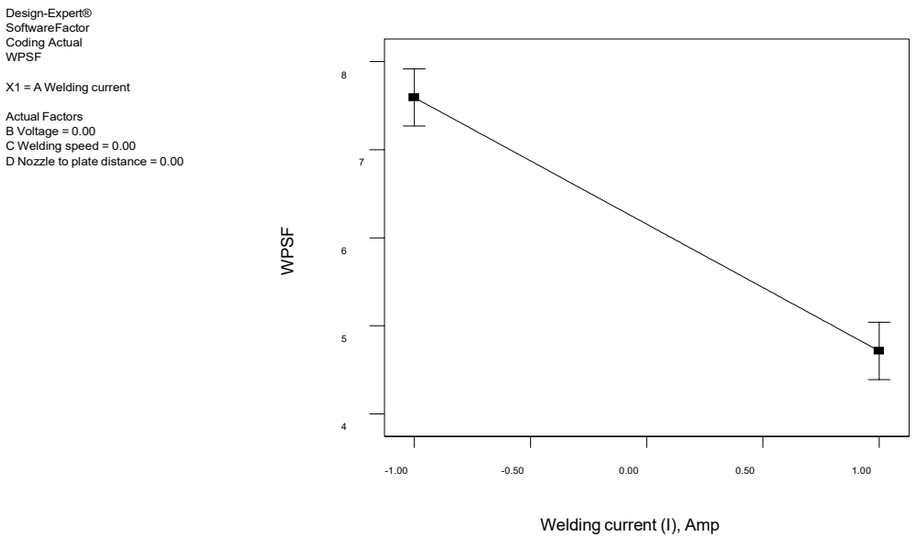

Fig. 4 Main effect of welding current on WPSF

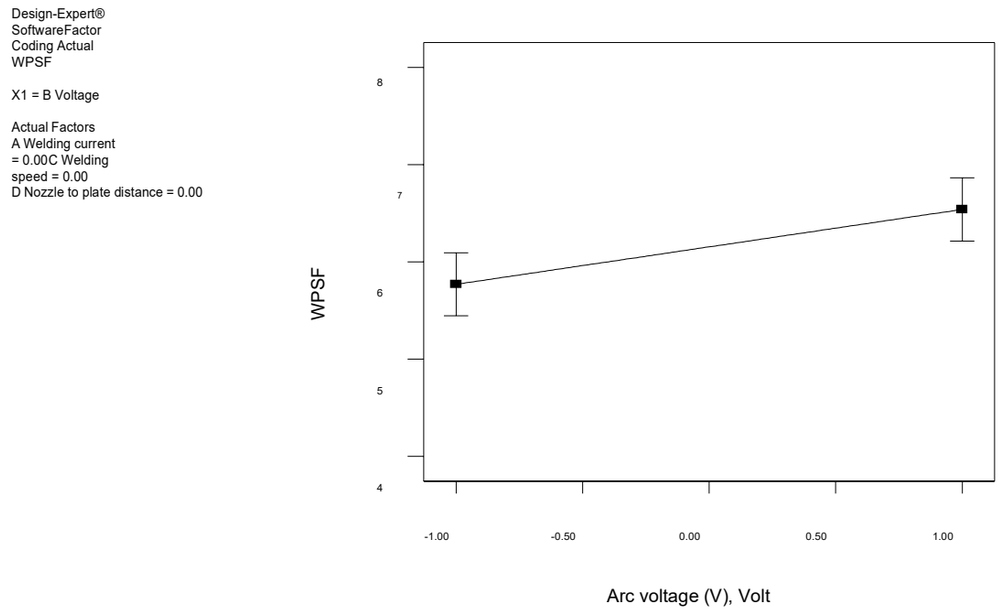

Fig. 5 Main effect of arc voltage on WPSF

Journal of Manufacturing Engineering, ISSN: 0973-6867, December 2024, Vol. 19, Issue. 4, pp 108-125
DOI: https://doi.org/10.37255/jme.v19i4pp108-125

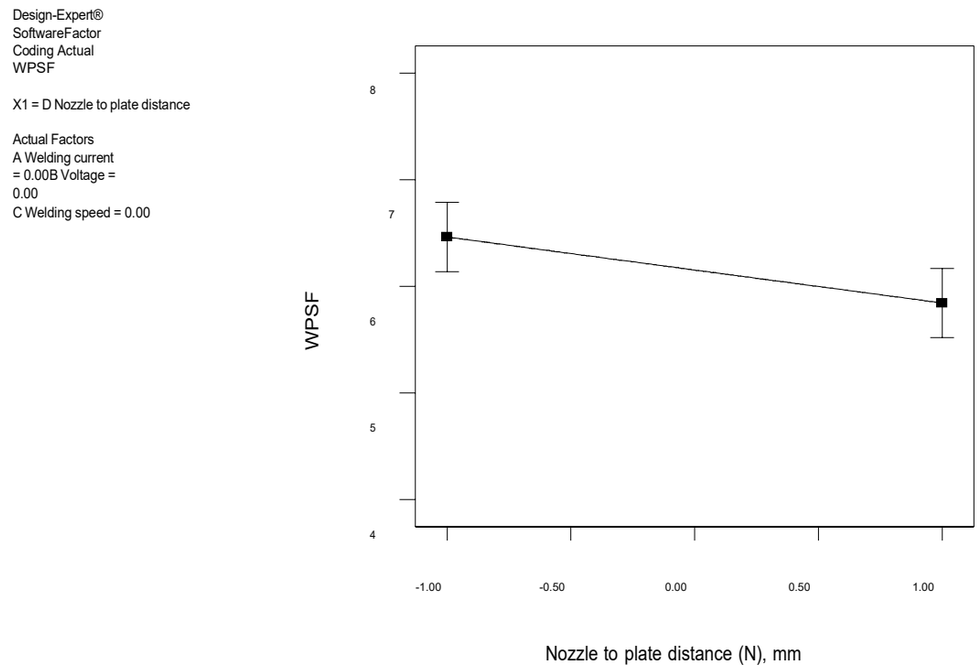

Fig. 6 Main effect of the nozzle-to-plate distance on WPSF

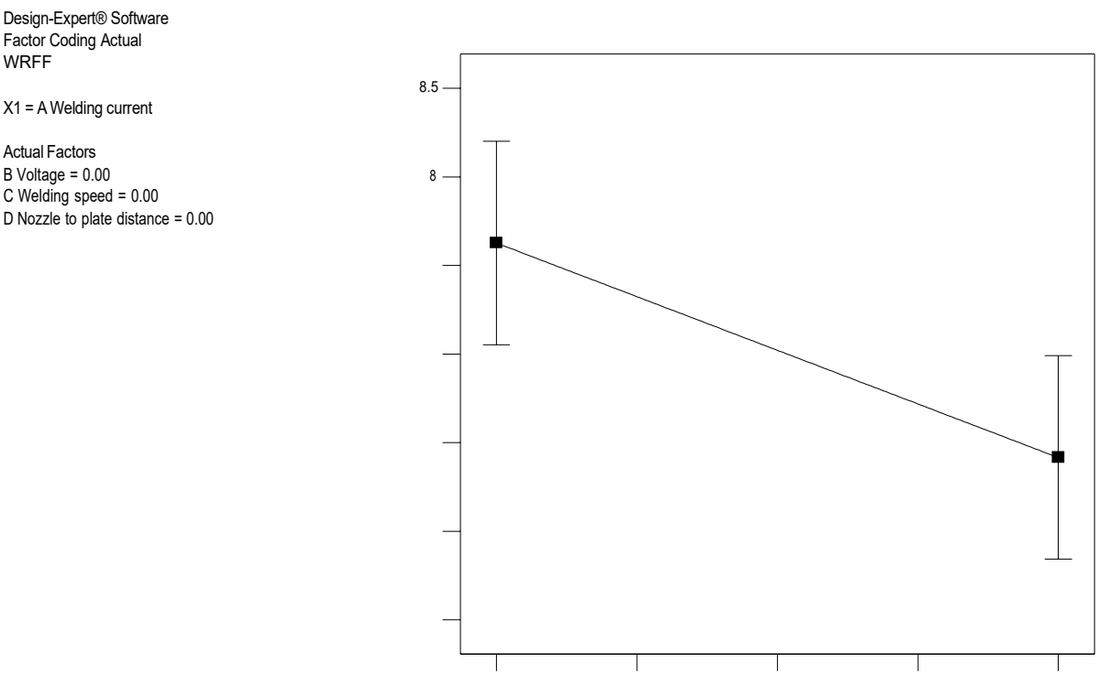

Fig. 7 Main effect of welding current on WRFF

Journal of Manufacturing Engineering, ISSN: 0973-6867, December 2024, Vol. 19, Issue. 4, pp 108-125
DOI: https://doi.org/10.37255/jme.v19i4pp108-125

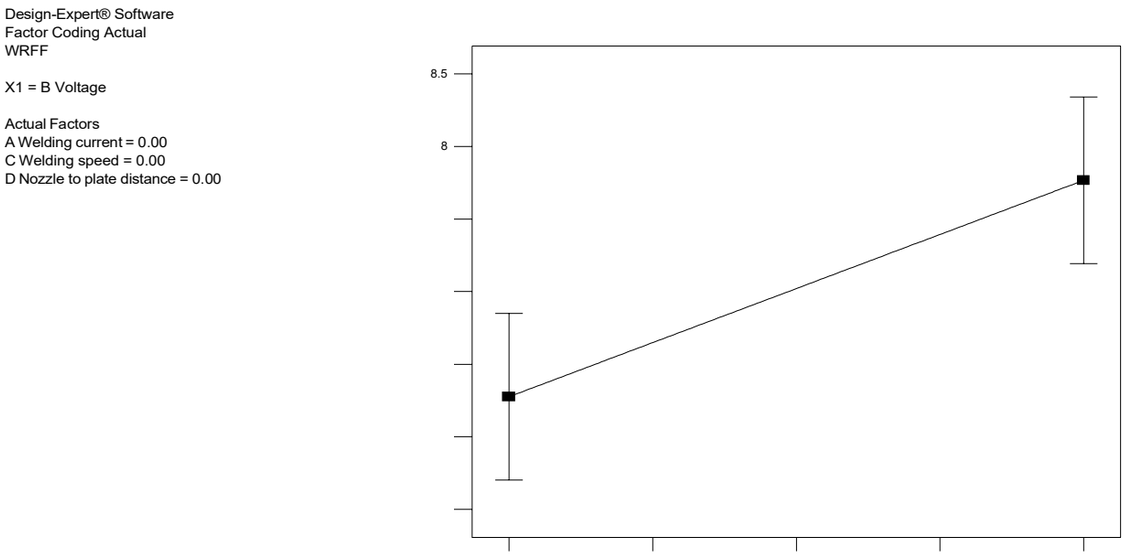

Fig. 8 Main effect of arc voltage on WRFF

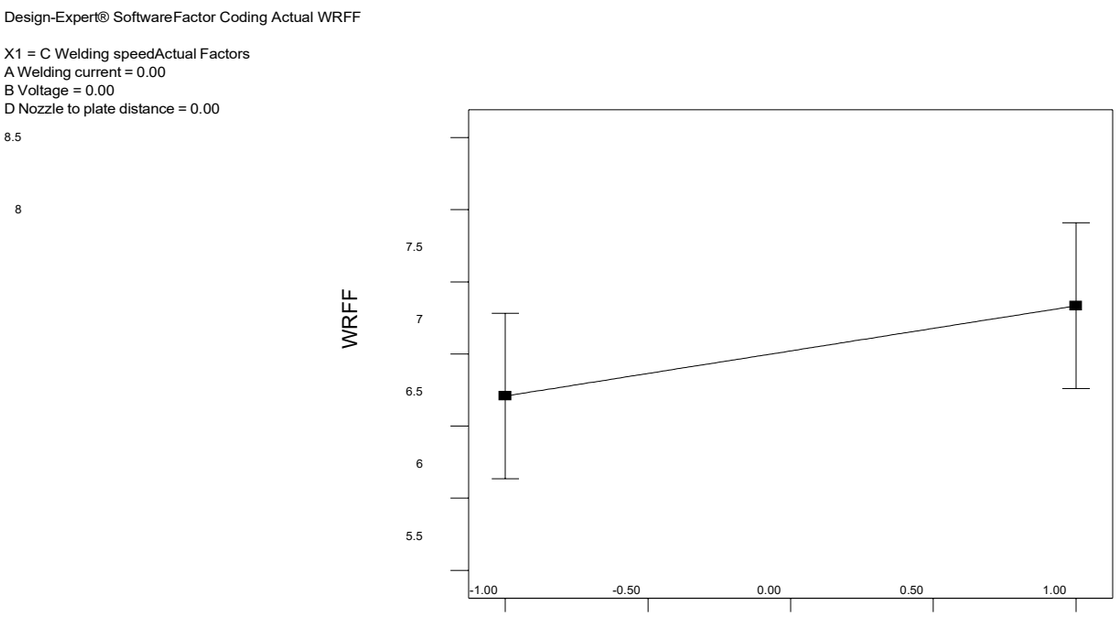

Fig. 9 Main effect of welding speed on WRFF

Journal of Manufacturing Engineering, ISSN: 0973-6867, December 2024, Vol. 19, Issue. 4, pp 108-125
DOI: https://doi.org/10.37255/jme.v19i4pp108-125

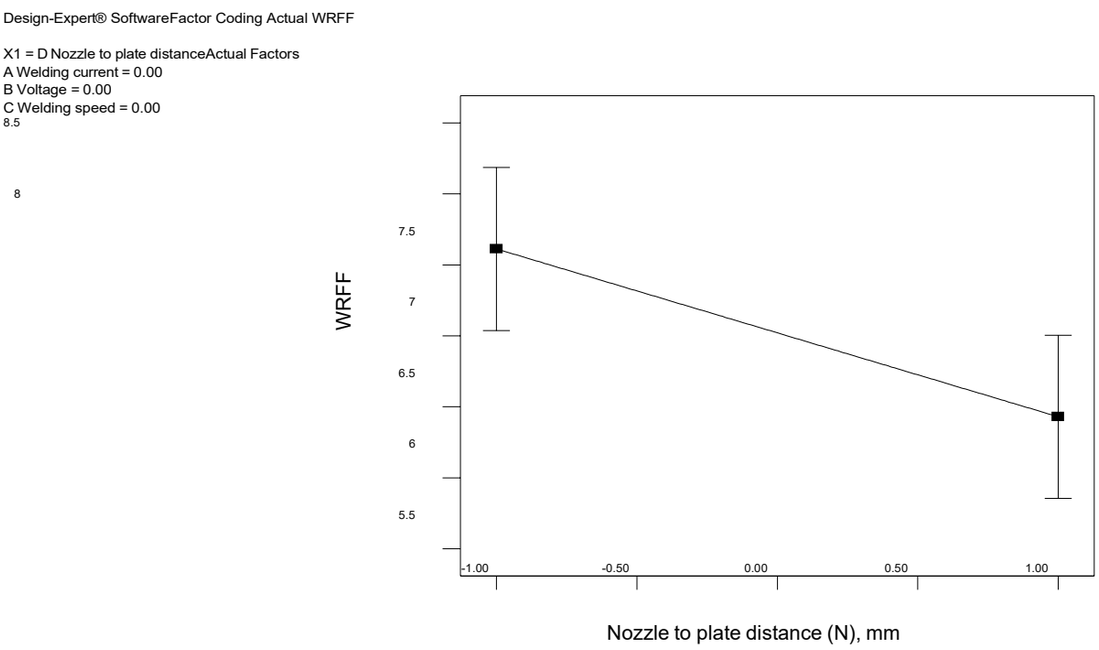

Fig. 10 Main effect of the nozzle to plate distance on WRFF

3.1 Main Effect of Process Variables on WRFF

Weld reinforcement form factor (WRFF) rises as welding speed and arc voltage increase but falls as welding current and nozzle-to-plate distance increase, as illustrated in Fig. 7-10.

3.2 Main Effect of Process Variables on % Dilution

The percentage dilution rises as welding speed and arc voltage increase but falls as a nozzle-to-plate distance increases, as seen in Fig. 11-13. Welding current has no discernible impact on the percentage of dilution.

3.3 Main Effect of Process Variables on Total Bead Volume

Fig. 14-17 demonstrates that while the total bead volume reduces as welding speed, arc voltage, and nozzle-to-plate distance rise, it increases with welding current.

3.4 Interaction Effect of Welding Current and Arc Voltage on WPSF

Fig. 18 shows that, for all arc voltage values, the weld penetration shape factor (WPSF) falls as the welding current increases; nevertheless, the fall rate increases with increasing arc voltage. Fig. 19 displays the response surface due to the welding current and arc voltage interaction on the weld penetration shape factor.

3.5 Interaction Effect of Welding Current and Arc Voltage on WRFF

Fig. 20 shows that the weld reinforcement form factor (WRFF) falls at low arc voltage values as welding current increases, but it grows at high arc voltage values. So, arc voltage positively affects weld reinforcement form factor while welding current has a negative effect. Fig. 21 displays the response surface due to the interaction between welding current and arc voltage on WRFF.

3.6 Interaction Effect of Welding Current and Arc Voltage on % Dilution

Fig. 22 shows that the dilution percentage rises as the welding current increases at high arc voltage values but falls as the current increases at low arc voltage values. Thus, welding current hurts the dilution percentage, but arc voltage has a beneficial effect. Fig. 23 displays the response surface due to the interaction between welding current and arc voltage on the dilution percentage.

Journal of Manufacturing Engineering, ISSN: 0973-6867, December 2024, Vol. 19, Issue. 4, pp 108-125
DOI: https://doi.org/10.37255/jme.v19i4pp108-125

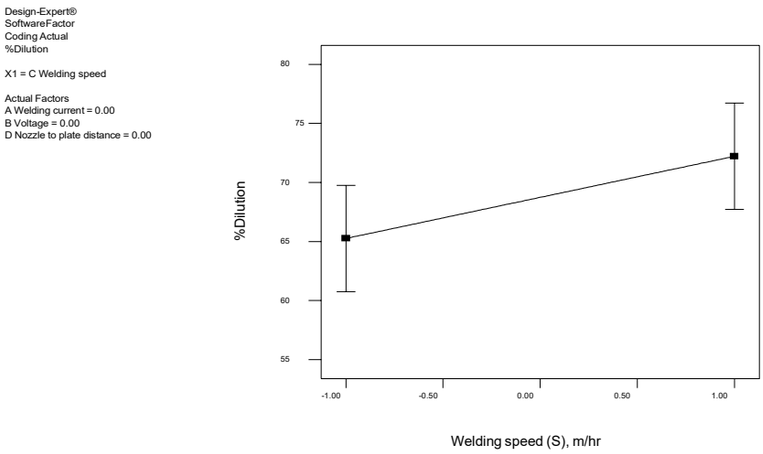

Fig. 11 Main effect of welding current on % Dilution

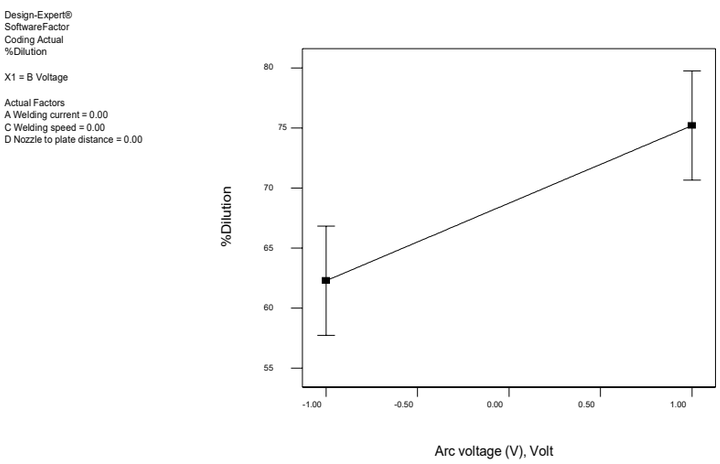

Fig. 12 Main effect of arc voltage on % Dilution

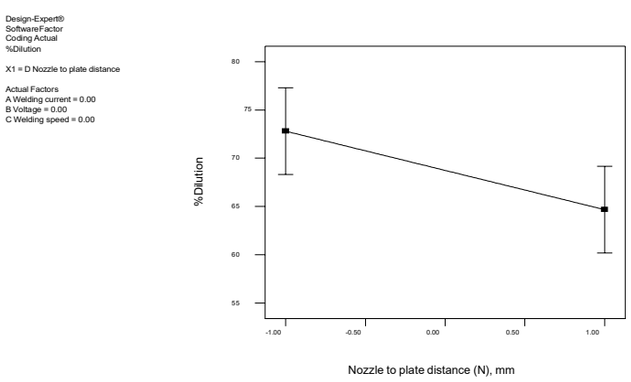

Journal of Manufacturing Engineering, ISSN: 0973-6867, December 2024, Vol. 19, Issue. 4, pp 108-125
DOI: https://doi.org/10.37255/jme.v19i4pp108-125

Fig. 13 Main effect of nozzle to plate distance on % Dilution

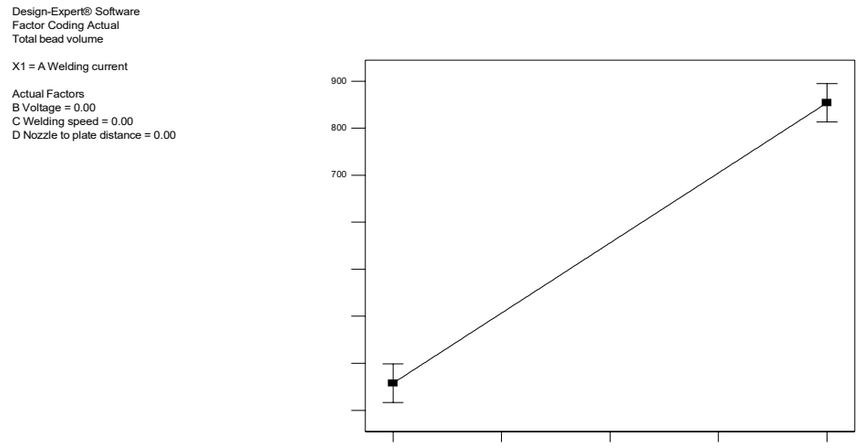

Fig. 14 Main effect of welding current on total bead volume

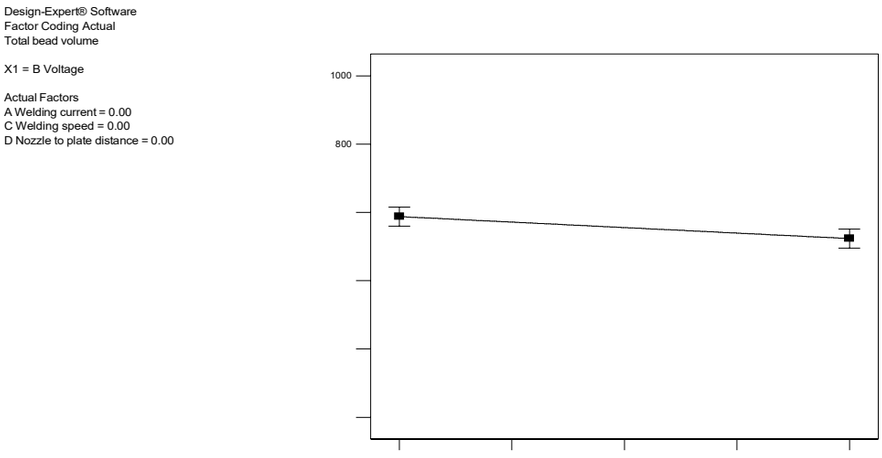

Fig. 15 Main effect of arc voltage on total bead volume

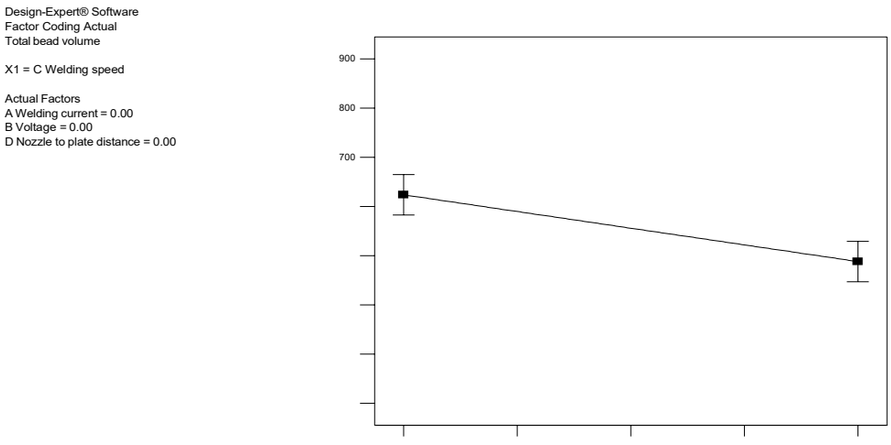

Journal of Manufacturing Engineering, ISSN: 0973-6867, December 2024, Vol. 19, Issue. 4, pp 108-125
DOI: https://doi.org/10.37255/jme.v19i4pp108-125

Fig. 16 Main effect of welding speed on total bead volume

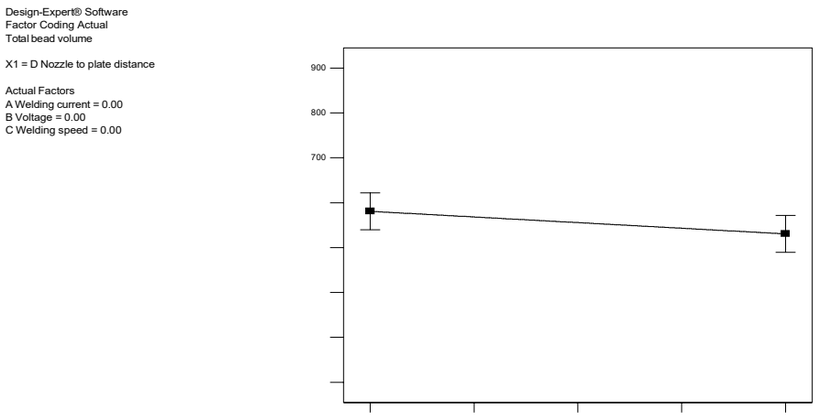

Fig. 17 Main effect of nozzle-to-plate distance on total bead volume

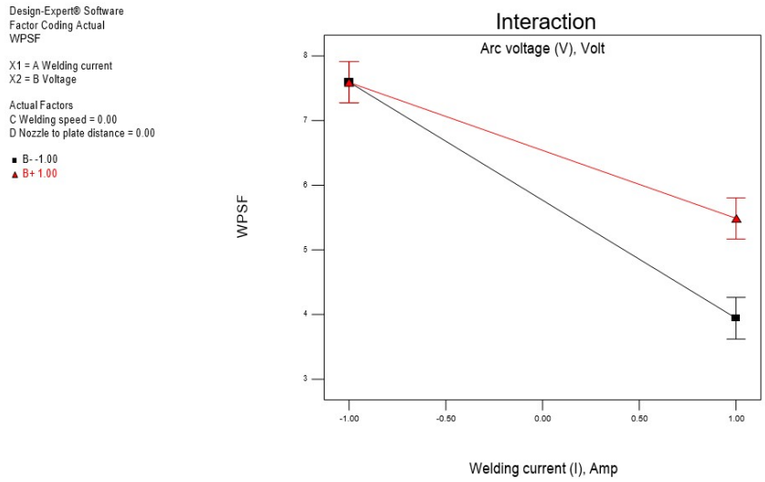

Fig. 18 Interaction effect of welding current and arc voltage on WPSF

Journal of Manufacturing Engineering, ISSN: 0973-6867, December 2024, Vol. 19, Issue. 4, pp 108-125
DOI: https://doi.org/10.37255/jme.v19i4pp108-125

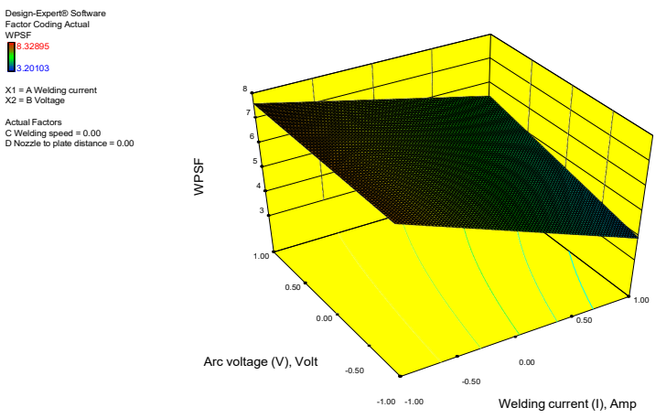

Fig 19 Interaction effect of welding current and arc voltage on WPSF (Response surface)

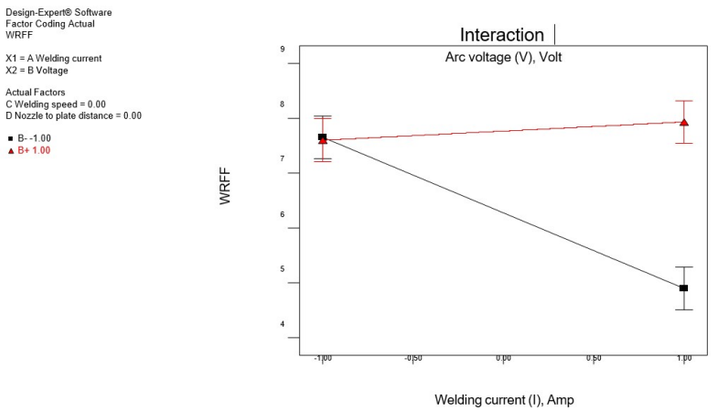

Fig. 20 Interaction effect of welding current and arc voltage on WRFF

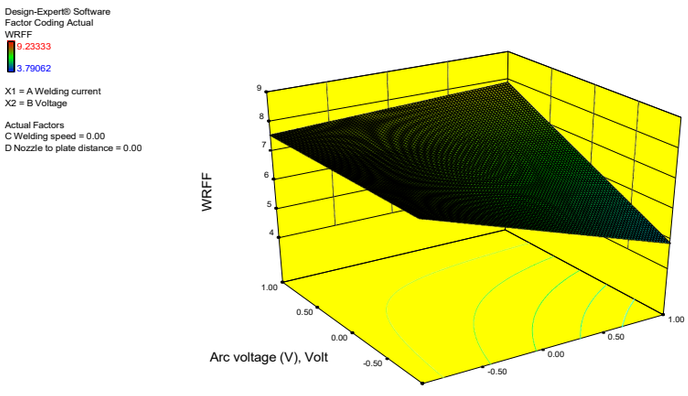

Fig 21 Interaction effect of welding current and arc voltage on WRFF (Response surface)

Journal of Manufacturing Engineering, ISSN: 0973-6867, December 2024, Vol. 19, Issue. 4, pp 108-125
DOI: https://doi.org/10.37255/jme.v19i4pp108-125

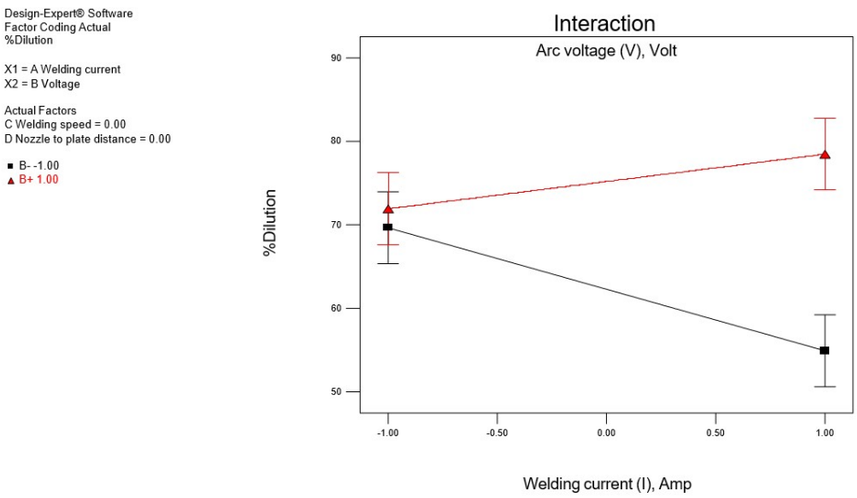

Fig. 22 Interaction effect of welding current and arc voltage on % dilution

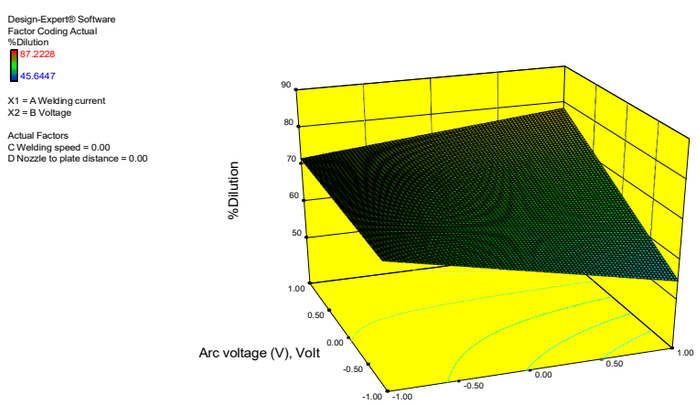

Fig 23 Interaction effect of welding current and arc voltage on % dilution (Response surface)

Journal of Manufacturing Engineering, ISSN: 0973-6867, December 2024, Vol. 19, Issue. 4, pp 108-125
DOI: https://doi.org/10.37255/jme.v19i4pp108-125

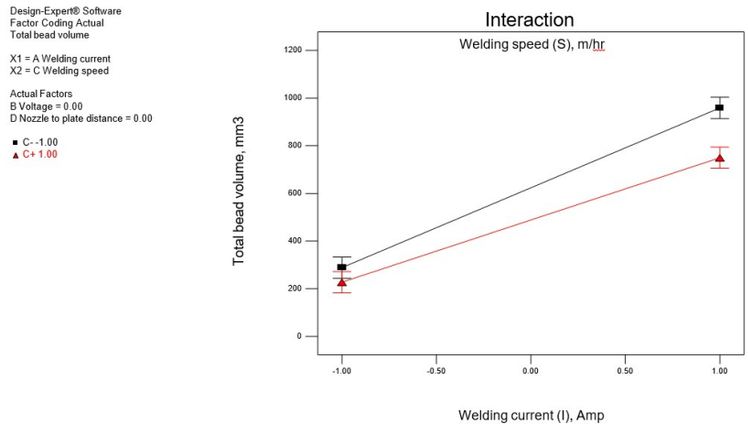

Fig. 24 Interaction effect of welding current and welding speed on total bead volume

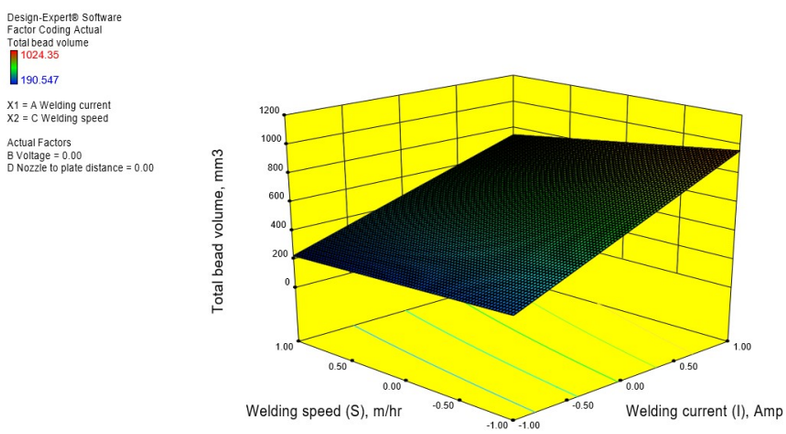

Fig 25 Interaction effect of welding current and welding speed on total bead volume (Response surface)

Journal of Manufacturing Engineering, ISSN: 0973-6867, December 2024, Vol. 19, Issue. 4, pp 108-125
DOI: https://doi.org/10.37255/jme.v19i4pp108-125

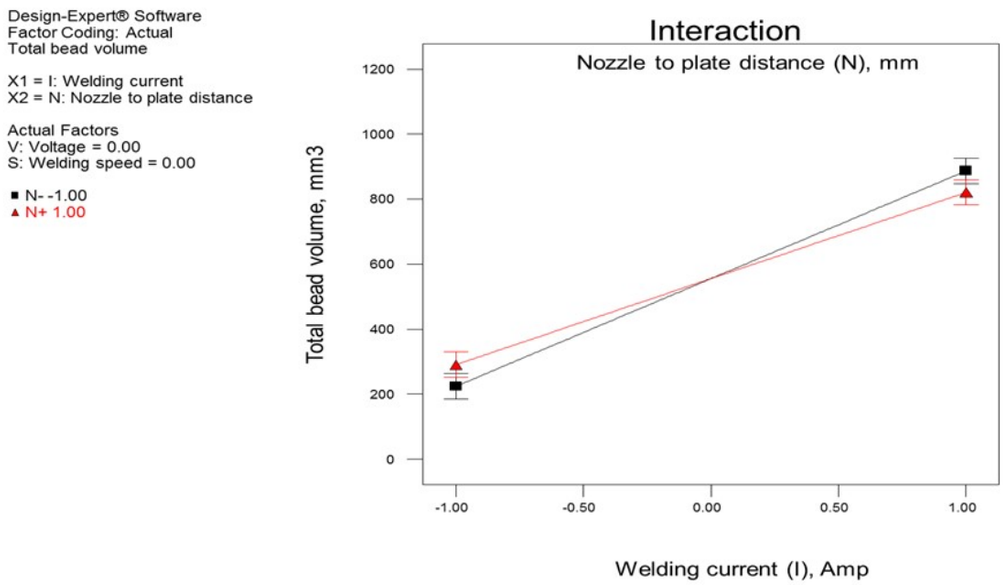

Fig 26 Interaction effect of welding current and nozzle to plate distance on total bead volume

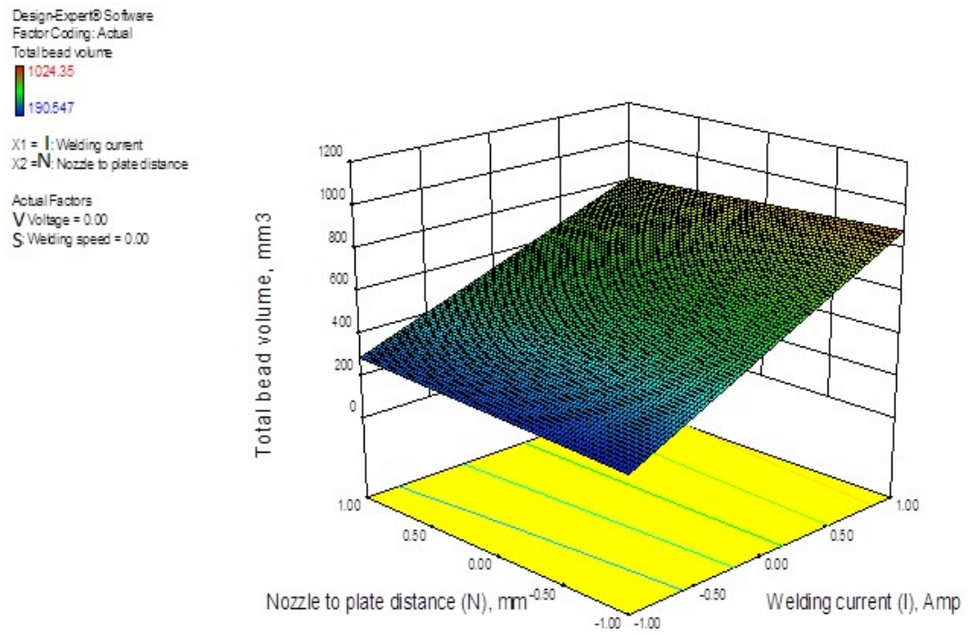

Fig 27 Interaction effect of welding current and nozzle to plate distance on total bead volume (Response surface)

3.7 Interaction Effect of Welding Current and Welding Speed on Total Bead Volume

Although the rate of increase is higher for low welding speed values, Fig. 24 illustrates that the total

bead volume increases as the welding current increases for all welding speed values. The response surface resulting from the interactions between welding speed and welding current on the overall bead volume is displayed in Fig. 25.

3.8 Interaction Effect of Welding Current and nozzle to plate distance on Total Bead Volume

Fig. 26 shows that the total bead volume rises as the welding current increases for all nozzle-to-plate distance values, although the rate of increase is marginally higher at low nozzle-to-plate distance values. Fig. 27 displays the response surface due to the interaction between the welding current and the distance between the nozzle and the plate on the overall bead volume.

4. Conclusions

i. Using design expert software and two-level half-factorial approaches, it is simple to create mathematical models that forecast weld bead parameters within the feasible range of process parameters for carbon steel SAW.

ii. The main effects of process variables and their interaction on weld bead parameters can be effectively measured using design expert software.

iii. Weld penetration shape factor and weld reinforcement form factor are negatively impacted by the welding current, although the total bead volume is positively impacted. It has no discernible impact on the dilution percentage.

iv. The arc voltage hurts the dilution percentage but has a favourable impact on the weld penetration shape factor, weld reinforcement form factor, and total bead volume.

v. Total bead volume is negatively impacted by welding speed, although WRFF and dilution percentage are positively affected. It doesn't significantly impact WPSF.

vi. The distance between the nozzle and the plate negatively impacts All bead characteristics, including WPSF, WRFF, % dilution, and total bead volume**.**

References

1. *O.P. Khanna, A Text Book of Welding Technology, Dhanpat Rai Publications Ltd., 2006.*

2. *S.V. Nandkarni, Modern Arc Welding Technology, Oxford & IBH Publishing Co. Pvt. Ltd., New Delhi, 1998.*

3. *D.C. Montgomery, Design and Analysis of Experiment, John Wiley, New York, NY. S.R. Gupta and N. Arora, "Influence of flux basicity on weld bead geometry and heat affected zone in submerged arc welding," Indian Welding Journal, vol. 24, no. 7, pp. 127–133, 1991.*

4. *L.J. Yang, M.J. Bibby, and R.S. Chandal, "AWS," Welding Journal, pp. 11–18, 1993.*

5. *V. Gunraj and N. Murugan, "Prediction and optimization of weld bead volume for the submerged arc process," Welding Journal, vol. 79, no. 11, pp. 331–338, 2000.*

6. *S. Pandey, "Welding current in submerged arc welding," Indian Welding Journal, 2003.*

7. *S. Kumanan, J.E. Dhas Raja, and K. Gowthaman, "Determination of submerged arc welding process parameters using Taguchi method and regression analysis," Indian Journal of Engineering & Materials Sciences, vol. 14, pp. 177–183, 2007.*

8. *S. Datta, A. Bandyopadhyay, and P.K. Pal, "Modeling and optimization of features of bead geometry including percentage dilution in submerged arc welding using a mixture of fresh flux and fused slag," International Journal of Advanced Manufacturing Technology, vol. 36, pp. 1080–1090, 2008.*

9. *S.P. Tewari, A. Gupta, and J. Prakash, "Effect of welding parameters on the weldability of material," International Journal of Engineering Science and Technology, vol. 2, no. 4, pp. 512–516, 2010.*

10. *V. Kumar, "Modeling of weld bead geometry and shape relationship in submerged arc welding using developed fluxes," Jordan Journal of Mechanical and Industrial Engineering, vol. 5, no. 5, 1995–6665, 2011.*

11. *D.K. Choudhary, "To study the effect of welding parameters on weld bead geometry in SAW welding process," Elixir Mechanical Engineering, vol. 40, pp. 5519–5524, 2011.*